RESEARCH PAPER

Vacuolar processing enzyme (VPE) activates programmed cell death in the apical meristem inducing loss of apical dominance

Paula Teper-Bamnolker[1*], Yossi Buskila[1,2*], , Eduard Belausov[3], Dalia Wolf[4], Adi Doron-Faigenboim[5], Shifra Ben-Dor[6], Renier A. L. Van der Hoorn[7], Amnon Lers[1] and Dani Eshel[1,†]

[1] Department of Postharvest and Food Sciences, ARO, The Volcani Center, Rishon LeZion, Israel; [2] The Robert H. Smith Institute of Plant Sciences and Genetics in Agriculture, The Hebrew University of Jerusalem, Robert H. Smith Faculty of Agriculture Food and Environment, Rehovot, Israel; [3] Department of Ornamental Horticulture, ARO, The Volcani Center, Rishon LeZion, Israel; [4] Department of Vegetables and Field Crops, ARO, The Volcani Center, Rishon LeZion, Israel; [5]Institute of Plant Sciences, ARO, The Volcani Center, Rishon LeZion, Israel; [6] Department of Biological Services, Weizmann Institute of Science, Rehovot, Israel; [7] Plant Chemetics Laboratory, Department of P, University of Oxford, Oxford, UK.

[*]These authors contributed equally to this work

Author for correspondence: Dani Eshel

Tel: +972 50 6220621

E-mail: dani@agri.gov.il

Total word count: 5,144 (introduction: 533, Material and Methods: 2,098, Results 1,986, Discussion: 990, Acknowledgements: 64)

Number of figures: 5

Supporting information: yes

The date of submission: December 13, 2016; Manuscript contain: 0 tables and 5 figures; Total word count:8,016; Supplementary Data: 3 tables and 3 figures.

Suggested short running title: VPE controls stem branching

ABSTRACT

The potato (*Solanum tuberosum* L.) tuber is a swollen underground stem that can sprout in an apical dominance (AD) pattern. Bromoethane (BE) induces loss of AD and the accumulation of vegetative vacuolar processing enzyme (StVPE) in the tuber apical meristem (TAM). VPE activity, induced by BE, is followed by programmed cell death in the TAM. In this study, we found that the mature StVPE1 protein (mVPE) exhibits specific activity for caspase-1, but not caspase-3 substrates. Optimal activity of mVPE was achieved at acidic pH, consistent with localization of StVPE1 to the vacuole, at the edge of the TAM. Downregulation of St*VPE1* by RNAi resulted in reduced stem branching and retained AD in tubers treated with BE. Overexpression of St*VPE1* fused to GFP showed enhanced stem branching after BE treatment. Our data suggest that, following stress, induction of St*VPE1* in the TAM induces AD loss and stem branching.

Key words: Apical dominance (AD), caspase, *Solanum tuberosum* (potato), stem branching, tuber apical meristem (TAM), vacuolar processing enzyme (VPE).

INTRODUCTION

The tuber of potato (*Solanum tuberosum* L.) is a swollen underground stem. Once formed, potato tubers undergo a period of dormancy during which visible bud growth is inhibited. The length of the dormancy period, between 1 and 15 weeks, depends on the cultivar, and on environmental, physiological and hormonal changes that occur during storage (Burton, 1989, Sonnewald & Sonnewald, 2014). After dormancy release, tuber sprouting is usually initiated from its apical bud, which becomes dominant and inhibits the growth of the other tuber buds (Buskila, Sela, Teper-Bamnolker, Tal, Shani, Weinstain, Gaba, Tam, Lers & Eshel, 2016, Suttle, 2004, Teper-Bamnolker, Buskila, Lopesco, Ben-Dor, Saad, Holdengreber, Belausov, Zemach, Ori, Lers & Eshel, 2012). Exposing the tuber to abiotic stress, such as cold or hot storage or specific chemicals, leads to early sprouting and loss of apical dominance (AD) (Buskila *et al.*, 2016, Eshel & Teper-Bamnolker, 2012).

Induction of early sprouting and loss of AD following application of the chemical bromoethane (BE) have been extensively studied. BE shortens the natural dormancy period from 2–4 months to approximately 10 days in cvs. Chacasina and Russett Burbank (Alexopoulos, Aivalakis, Akoumianakis & Passam, 2009, Campbell, Segear, Beers, Knauber & Suttle, 2008, Destefano-Beltran, Knauber, Huckle & Suttle, 2006), and induces type I loss of AD followed by type III loss of dominance expressed as excessive branching of the growing shoots. Type I is loss of dominance of the apical buds over those situated more basipetally on the tuber.

Type III is loss of dominance of the developing sprout over its own branching, meaning that the side stems do not emerge from the base of the sprout as in type II (Teper-Bamnolker *et al.*, 2012). Campbell *et al.* (2008) observed that transcript profiles during BE-induced cessation of dormancy are similar to those observed in natural dormancy release, suggesting that both follow a similar biological pattern during this transition. Thus, BE treatment can be used to compress and synchronize release from the dormant period, which is an advantage from an experimental standpoint (Campbell *et al.*, 2008, Eshel, 2015).

We previously proposed that programmed cell death (PCD) in the tuber apical meristem (TAM) is one of the mechanisms regulating AD (Teper-Bamnolker *et al.*, 2012). PCD plays an important role in various stages of plant development, such as embryogenesis, self-incompatibility, xylogenesis and senescence, and in the response to biotic or abiotic stresses (Gunawardena & McCabe, 2015, Kabbage, Kessens, Bartholomay & Williams, 2017, Van Hautegem, Waters, Goodrich & Nowack, 2015). Hallmarks of PCD identified in the TAM during normal growth were more extensive when AD was lost following either extended cold storage or BE treatment (Eshel & Teper-Bamnolker, 2012). Hallmarks for PCD in the TAM include DNA fragmentation and structural modifications of the cell vacuole followed by upregulation of the vacuolar processing enzyme gene (*VPE1*) and elevated VPE activity (Teper-Bamnolker *et al.*, 2012). Treatment of tubers with BE followed by application of caspase-1 inhibitor repressed the loss of AD, suggesting that VPE activity is associated with promoting the loss of AD (Teper-Bamnolker *et al.*, 2012).

The VPE proteins belong to a family of cysteine proteinases that are well conserved among a variety of organisms, including many plant and animal species (Cai & Gallois, 2015, Hatsugai, Yamada, Goto-Yamada & Hara-Nishimura, 2015,

Sueldo & van der Hoorn, 2017). Hatsugai et al. (2004) reported that VPE can cleave caspase-specific substrates and is required for cell-death activation by tobacco mosaic virus. Despite the limited sequence identity with caspase-1, VPE proteins share similar substrate specificity, and their involvement in the maturation process of seed storage proteins has been reported (Hatsugai *et al.*, 2015, Lu, Chandrasekar, Oeljeklaus, Misas-Villamil, Wang, Shindo, Bogyo, Kaiser & van der Hoorn, 2015, Shimada, Yamada, Kataoka, Nakaune, Koumoto, Kuroyanagi, Tabata, Kato, Shinozaki & Seki, 2003). Thus, VPEs are involved in several functional aspects in plants; however, the role of VPE in the regulation of AD has not been demonstrated.

In this work, we show, for the first time, that silencing and overexpression of VPE in transgenic potato plants respectively represses and induces AD. Based on our analyses of VPE accumulation, and subcellular and tissue-specific localization in response to chemical stress, we propose that VPE activation in the TAM stimulates the loss of AD.

MATERIALS AND METHODS

Plant material

Potato (*S. tuberosum* L.) cv. Désirée, grown in the northern Negev, Israel, under standard field conditions was used for the entire study. Harvested tubers were cured for 2 weeks, with a gradual temperature reduction from 25ºC to 4ºC; they were then stored in the dark at 4ºC in 95% humidity generated by an ultrasonic humidifier (SMD Technology, Rehovot, Israel).

BE treatments

BE treatments were performed as described by Law and Suttle (2003). Each treatment contained three replicates of four glass chambers containing 10 tubers each, for a total of 120 tubers, which were sealed and exposed to filter paper soaked with 0.2 mL BE (Sigma) per liter of container volume. The sealed glass chambers were incubated for 24 h at room temperature in the dark. After treatment, tubers were placed in a chemical hood for 4 h at room temperature (to allow the release of absorbed BE vapors) and subsequently stored at 14ºC in the dark in 85% humidity. Using a cork borer (Ø 0.5 cm, 3-mm penetration), the apical complex was excised at several time points: immediately after treatment (24 h), and 48 and 72 h after treatment. Excised meristems were immediately frozen in liquid nitrogen and stored at -80ºC for later measurements of VPE activity and AMS101 labeling.

Gene construction

In the *S. tuberosum* genome, three VPE genes (St*VPE1*, ACC68680; St*VPE2*, ACC68681 and St*VPE3*, XP006342509) were available in the NCBI database (NCBI http://www.ncbi.nlm.nih.gov/dbEST). To define the whole family, TBLASTN searches with the protein sequence were performed against the *Solanum phureja* genome scaffolds (DM_V3) (http://potatogenomics.plantbiology.msu.edu), and nine putative protein-encoding genes and two putative pseudogenes were defined (Altschul, Madden, Schäffer, Zhang, Zhang, Miller & Lipman, 1997). Tomato sequences were taken from the Solgenomics website: http://solgenomics.net/ according to the accession numbers of Sl*VPE*1–14 published by (Wang, Cai, Wang, Tian & Qin, 2017).

Phylogenetic analysis

Thirty-five VPE sequences were aligned using the MAFFT program (http://mafft.cbrc.jp/alignment/server/ version 7) with default parameters. A maximum likelihood tree with 100 bootstrap replicates using PhyML 3.0 software (Guindon, Dufayard, Lefort, Anisimova, Hordijk & Gascuel, 2010) was constructed based on the LG matrix-based model (Le & Gascuel, 2008). The tree was graphically designed using FigTree version 1.4.2 (http://tree.bio.ed.ac.uk/software/figtree/).

VPE activity

VPE activity was measured using the method reported by Kuroyanagi et al. (2002) with some modifications. Frozen apical meristems were harvested and homogenized in extraction buffer (50 mM sodium acetate pH 5.5, 50 mM NaCl, 1 mM EDTA, and 100 mM dithiothreitol [DTT]) under ice-cold conditions. The homogenate was centrifuged at 15,000*g* for 15 min at 4ºC, and the supernatant was used for the enzyme assay. To determine optimal pH for protein activity, proteins were extracted in 50 mM citrate phosphate buffer, supplemented with 50 mM NaCl, 1 mM EDTA, and 100 mM DTT, in a pH range of 4 to 7.5. Aliquots of 80 µM N-acetyl-Glu-Ser-Glu-Asp-4-methylcoumaryl-7-amide (Ac-ESEN-MCA), N-acetyl-Tyr-Val-Ala-Asp-4-methylcoumaryl-7-amide (Ac-YVAD-MCA) or N-acetyl-Asp-Glu-Val-Asp-4-methylcoumaryl-7-amide (Ac-DEVD-MCA) (Peptide Institute, Osaka, Japan) were used as the substrates for the reactions, and the amount of 7-amino-4-methylcoumarin released was determined spectrophotometrically at an excitation wavelength of 380 nm and an emission wavelength of 460 nm (Enspire 2003 Multi Label Reader, Perkin-Elmer) at room temperature. A known amount of 7-amino-4-methylcoumarin was used for calibration. To confirm that the hydrolyzing activity

was from VPE, 80 μM Ac-Tyr-Val-Ala-Asp-1-aldehyde (Ac-YVAD-CHO; Peptide Institute), which specifically inhibits VPE (Hatsugai *et al.*, 2004, Mino, Murata, Date & Inoue, 2007), or N-biotin-Asp-Glu-Val-Asp-aldehyde (biotin-DEVD-CHO; Enzo Life Sciences, BVBA, Zandhoven, Belgium) was added to the reaction mixture. Protein content was determined with the Pierce™ 660nm Protein Assay Reagent (Thermo Scientific) using bovine serum albumin (BSA) as the standard.

AMS101 labeling

Labeling was performed as previously reported by Misas-Villami et al. (2013). Briefly, we incubated approximately 100 μg protein in buffer containing 50 mM sodium acetate (NaOAc) pH 5.5, 100 mM DTT and 1.5 μM AMS101 for 2 h at room temperature (22–25ºC) in the dark. The labeling reaction was stopped by adding SDS–PAGE loading buffer containing DTT, and the reaction mixture was separated on a 4–12% SDS gel (PAGEgel, Expedeon, CA). Labeled proteins were visualized by in-gel fluorescence scanning using a Typhoon 9000 scanner (GE Healthcare, http://www.gelifesciences.com) with excitation and emission at 532 and 580 nm, respectively. Inhibition assays were performed by preincubating protein extracts with 300 μM Ac-YVAD-CHO or biotin-DEVD-CHO for 30 min before labeling.

Biotinylated-inhibitor blot analysis

In-vitro analysis of proteins was performed as previously reported by Hatsugai et al. (2004). Briefly, partially purified proteins were incubated with biotin-X-Tyr-val-Ala-Asp-fluoromethyl ketone (biotin-XVAD-fmk; Calbiochem) at 20 μM final concentration (1 h, room temperature). The biotin-xVAD-fmk-conjugated enzyme was subjected to 4–20% SDS-PAGE and transferred to a pure nitrocellulose

membrane (Whatman). The membrane was treated with a blocking solution without milk (10 mM Tris pH 7.5, 2% w/v BSA, 0.5% w/v NP40 and 0.1% w/v Tween 20) and then with streptavidin-conjugated horseradish peroxidase (diluted 5000-fold; Pierce) overnight. Detection was performed with enhanced chemiluminescence (SuperSignal West Pico Chemiluminescent Substrate, Thermo Scientific).

RNA-interference (RNAi) construct

A 500-bp cDNA fragment was amplified from the St*VPE1* gene (accession no. EU605871) using a forward primer including XbaI–XhoI sites 5'-cga*tctagactcgag*CTGCTCTCCTTGGGAACAAAA-3' and a reverse primer including EcoRI–BamHI sites 5'-cac*ggatccgaattc*TGACATGTGAACCATAGGCAGG-3' (restriction sites in italics and underlined). The PCR product was digested with XhoI–EcoRI for sense and BamHI–XbaI for antisense fragments and cloned into the pHANNIBAL vector at the respective sites (Wesley, Helliwell, Smith, Wang, Rouse, Liu, Gooding, Singh, Abbott, Stoutjesdijk, Robinson, Gleave, Green & Waterhouse, 2001) under the constitutive CaMV 35S promoter, with two sets of multiple cloning sites flanking an intron from the pyruvate orthophosphate dikinase gene (*PDK*), and the *Agrobacterium tumefaciens* octopine synthase (OCS) terminator. The resulting RNAi construct containing the inverted repeat configuration of the 500-bp fragment was introduced into *Escherichia coli* JM109 competent cells (Promega). DNA plasmid was extracted with GenElute™ Kit (Sigma-Aldrich) and validated using the restriction enzymes BamHI and NotI. The resulting plasmid was verified by sequencing (Hylabs, Rehovot, Israel). The RNAi cassette was released from pHANNIBAL by NotI, and subcloned using T4-ligase (Fermentas) into binary vector pART27 (Gleave, 1992). The recombinant binary vector pART27 was introduced

into the competent *A. tumefaciens* strain EHA105 by freeze-thaw method (Weigel & Glazebrook, 2006) using spectinomycin selection (Sigma-Aldrich). For cloning validation, we amplified a fragment using a forward primer from the CaMV 35S promoter 5'- AATCCCACTATCCTTCGCAAGACC-3', and the original primer used for cloning (containing the EcoRI–BamHI sites) was used as the reverse primer. For antisense validation, we amplified a fragment using primers from the PDK intron as forward 5'-GTCGAACATGAATAAACAAGGTA-3' and OCS terminator as reverse 5'-TTCAATTCTGTTGTGCACG-3' flanking the antisense fragment.

Plant transformation and transgenic selection

Potato leaves (cv. Désirée) were used for *Agrobacterium*-mediated leaf disc infection as described previously (Horsch, Rogers & Fraley, 1985, Rocha-Sosa, Sonnewald, Frommer, Stratmann, Schell & Willmitzer, 1989). Transgenic plants were selected on 25 mg/L kanamycin (Duchefa). For transgenic plant validation, PCR was performed using the primers described for the cloning validation. Ten independent lines were transferred to soil and grown at 25ºC in a greenhouse. After 100 days, tubers were harvested and stored at 4ºC in 95% humidity for further analysis. Five tubers from each plant, three plants from each transgenic line, were analyzed in each treatment.

mRNA regulation analysis

To validate RNAi-transgenic lines, plants were treated with 200 µL BE in a 2-L jar for 24 h as previously described (Teper-Bamnolker *et al.*, 2012). Leaves from at least 10 treated plants were collected 72 h after treatment and immediately frozen in liquid nitrogen. RNA was isolated from 100 mg ground tissue using Spectrum™

Plant Kit (Sigma-Aldrich). RNA samples were treated with Turbo DNase (Ambion) to remove contaminating DNA according to the manufacturer's protocol. cDNA was synthesized from 1.5 µg of total potato RNA using the Verso™ cDNA Kit (ABgene) according to the manufacturer's specifications. Quantitative real-time RT-PCR analysis of potato cDNA was performed as previously described (Teper-Bamnolker *et al.*, 2012). Briefly, quantitative real-time RT-PCR was performed using the ABsolute QPCR SYBR Green Mix Kit (ABgene). For the VPE gene, forward 5'-CTCGCATGGAATTGTCATCATA-3' and reverse 5'-GCATTTCTGGTACAAGTTCCACA-3' primers were used. As a housekeeping gene, ubiquitin 3 (accession no. L22576) was analyzed using the forward 5'-TTCCGACACCATCGACAATGT-3' and reverse 5'-CGACCATCCTCAAGCTGCTT-3' primers. Lines with different expression levels were grown for tuber production and sprouting analysis.

Tuber sprouting assay for potato RNAi lines

Harvested tubers were cured at 20ºC for 1 week, and then stored at 4ºC in 95% humidity generated by an ultrasonic humidifier (SMD Technology) for 40 days. Tubers were treated with BE as described above and sprouting buds were counted 6, 12, 20, 36, and 76 days after treatment. Buds were defined as sprouting when they reached 3 mm in length. To induce type II branching, tubers that were incubated at 14ºC for 80 days and had one dominant sprout were treated with BE.

Subcellular protein localization

Green fluorescent protein (GFP)-fusion construct was designed from the full St*VPE1* cDNA sequence (ppVPEγ), without the C-terminal domain. The St*VPE*

open reading frame was amplified from the St*VPE1* gene (accession no. EU605871) using forward primer 5'-GGGGACAAGTTTGTACAAAAAAGCAGGCTATGAATCGTTCCATCGCCGGA-3' and reverse primer 5'-GGGGACCACTTTGTACAAGAAAGCTGGGTC AGTCAGCACCTCTGGACC-3', and cloned into the Gateway vector pDONOR221 by standard BP clonase2 reaction according to the Gateway cloning system (Invitrogen, Carlsbad, CA). The resulting plasmid structure was verified by sequencing (Hylabs, Rehovot, Israel) and then cloned by standard LR clonase2 reaction (Invitrogen) into the expression vector pK7FWG2 (Karimi, Depicker & Hilson, 2007), resulting in C-terminal GFP-fusion protein. The recombinant binary vector was introduced into the competent *A. tumefaciens* strain EHA105 by the electroporation method (Weigel & Glazebrook, 2006) followed by spectinomycin selection of positive clones (Sigma-Aldrich). GFP was excited at 488 nm with an argon laser and visualized between 500 and 530 nm. A Leica SP8/LAS X laser scanning confocal microscope was used to observe fluorescently labeled cells. Image series (Z-stacks) were analyzed using the Bitplane Imaris software version 8.0.1 (Bitplane A.G.).

Histological analysis: terminal deoxynucleotidyl transferase-mediated dUTP nick end labeling (TUNEL) and 4'-6-diamidino-2-phenylindole (DAPI) staining

Histological analyses were performed 72 h after BE treatment using 10-mm thick TAM sections cut by microtome. Samples were stained as described previously (2012, Teper-Bamnolker, Dudai, Fischer, Belausov, Zemach, Shoseyov & Eshel, 2010). For TUNEL staining, fixed tissues were rehydrated with Histoclear and decreasing concentrations of ethanol (100%, 70%, and 30%). Tissue

permeabilization was performed with 20 μg/mL proteinase K (Gibco BRL) in 10 mM Tris, pH 7.5, at 37ºC for 30 min. After washing the tissue twice with phosphate-buffered saline (PBS), lysing enzyme (4 mg/mL) in 5 mM EDTA, pH 8, was added for 20 min with incubation at 37ºC. TUNEL reaction was performed on slides using the In Situ Cell Death Detection Kit with fluorescein (Roche Applied Science) according to the manufacturer's instructions. To visualize nuclei in meristem cells, samples were stained with DAPI (Sigma) at 1 mg/mL in PBS buffer for 10 min. For the positive control, we incubated fixed TAM tissue with DNase I (1500U/mL in 50 mM Tris-HCl, pH 7.5, 1 mg/mL BSA) for 10 min at 20ºC to induce DNA-strand breaks, prior to the labeling procedures. Negative and positive controls were treated identically except for omission of the enzyme solution (terminal deoxynucleotidyl transferase) or after incubation with DNAse I (Roche) for 30 min, respectively.

DAPI- and TUNEL-positive staining was observed with a Leica SP8/LAS X laser scanning confocal microscope. DAPI was excited with the 405-nm diode laser, and the emission was filtered with a BA 430- to 460-nm filter. TUNEL was excited with 488 nm of light, and the emission was filtered with a BA505IF filter.

RESULTS

StVPE1 is a vegetative-type VPE

VPEs are classified into three subfamilies: seed type, seed-coat type, and vegetative type, according to their protein sequence and expression pattern (Hatsugai *et al.*, 2015, Nakaune, Yamada, Kondo, Kato, Tabata, Nishimura & Hara-Nishimura, 2005, Wang, Duhita, Ariizumi & Ezura, 2016, Yamada, Shimada,

Nishimura & Hara-Nishimura, 2005). To characterize StVPE's developmental role, a phylogenetic study of the *VPE* gene family was performed followed by a biochemical study of the related protein.

In the *S. tuberosum* genome, three *VPE* genes (St*VPE1*, ACC68680; St*VPE2*, ACC68681 and St*VPE3*, XP006342509) were available in the NCBI database (NCBI http://www.ncbi.nlm.nih.gov/dbEST). As more *VPE* sequences could not be found in the available *S. tuberosum* genome, we looked for homologs in the genome of *S. phureja* (Sp) (http://potatogenomics.plantbiology.msu.edu), a perennial member of the *Solanum* genus in the family Solanaceae. Eleven *VPE* genes (two of them probably pseudogenes) were found in this genome (Consortium, 2011) (Supplementary Table S1 and Fig. S1). We named the Sp*VPE* genes Sp*VPE1–11* on the basis of their chromosomal location (Supplementary Table S1). Comparison between the genomic loci of the Solanaceae potato *VPE* genes and the tomato (*Solanum lycopersicum*; Sl) *VPE* genes *SlVPE1–14* (Wang et al., 2016) showed that they are very similar, with a large cluster on chromosome 8 containing all except two of the genes: Sp*VPE10* and Sl*VPE4*, which are located at a distal locus on chromosome 8, and Sp*VPE11 and* Sl*VPE5* on chromosome 12 (Fig. 1A and Supplementary Table S1).

Phylogenetic analysis showed that St*VPE1*, previously shown to be highly expressed in the TAM after 24 h of BE treatment (Teper-Bamnolker *et al.*, 2012), has high similarity to Sl*VPE3* and *5*, classified as vegetative-type (Kinoshita, Nishimura & Hara-Nishimura, 1995a) (Fig. 1B; gray color). Branch 2 contains seed-type *VPE*s and branch 3 includes seed-coat-type *VPE*s based on clustering with Sl*VPE4* and Sl*VPE1,2*, respectively *(*Ariizumi et al, 2011*)* (Fig. 1B; blue and yellow). Alignment of VPE protein sequences from *S. tuberosum*, *S. phureja* and *N.*

tabacum suggested that all StVPEs and SpVPEs contain signal peptides, N- and C-terminal propeptides and conserved amino acids which form the catalytic dyad (His and Cys) and substrate pocket (Arg and Ser) (Supplementary Fig. S2) (Hatsugai, Kuroyanagi, Nishimura & Hara-Nishimura, 2006, Misas-Villamil *et al.*, 2013). These results suggest that three St*VPE* and nine Sp*VPE* genes, classified in this study, encode proteins with features similar to those of other VPE proteins and might exhibit biochemical activity characteristic of VPE. Importantly, in this phylogenetic analysis, St*VPE1* was classified as vegetative type (branch 1), in accordance with its involvement in TAM growth and dominance.

BE treatment induces higher expression of the mature form of StVPE1 (mVPE) in the TAM

In a previous study, BE treatment was shown to induce early sprouting of dormant tubers and loss of AD. Hallmarks of PCD were observed in the TAM that correlated with the induced activity of StVPE1 (Teper-Bamnolker *et al.*, 2012). To determine whether BE treatment influences the level of mVPE, total TAM proteins were extracted 24, 48 and 72 h after BE treatment and detected using AMS101 labeling reagent. This reagent has been shown to specifically label the mature and active form of VPE (mVPE; Misas-Villamil *et al.*, 2013). Levels of mVPE protein increased as a result of 24 h BE treatment and during the 72 h after treatment initiation (Fig. 2A). This observation is consistent with StVPE1 upregulation (Teper-Bamnolker *et al.*, 2012) and demonstrates its processing into the active isoform (mVPE) during the first few days after treatment.

TAM mVPE has caspase-1 activity only under acidic conditions

Transcript levels of *StVPE1* are induced in potato TAM as a result of BE treatment (Teper-Bamnolker *et al.*, 2012). To determine the substrate specificity of TAM VPE in potato, we extracted total proteins from the TAM after 24 h of BE treatment (24 h of BE treatment; Teper-Bamnolker *et al.*, 2012). Proteins were partially purified by ion-exchange chromatography column and the VPE active fraction was collected (Teper-Bamnolker *et al.*, 2012).

We found that partially purified potato mVPE is active on the VPE-specific substrate Ac-ESEN-MCA (Hatsugai *et al.*, 2004, Kuroyanagi, Yamada, Hatsugai, Kondo, Nishimura & Hara-Nishimura, 2005, Teper-Bamnolker *et al.*, 2012) and the caspase-1 substrate Ac-YVAD-MCA (75.9% of the Ac-ESEN-MCA activity) (Fig. 2B). The caspase-1 inhibitor Ac-YVAD-CHO inhibited Ac-Glu-Ser-Glu-Asn-MCAase (ESENase) activity by 80% and Ac-Tyr-Val-Ala-Asp-MCAase (YVADase) activity by 67% (Fig. 2B). Furthermore, preincubation of mVPE with Ac-YVAD-CHO blocked labeling by AMS101, which specifically labels mVPE (Misas-Villamil *et al.*, 2013) (Fig. 2C). Using the caspase-3 substrate Ac-DEVD-MCA, only minor DEVDase activity (6.1% of the Ac-ESEN-MCA activity) was measured (Fig. 2B). The caspase-3 inhibitor Ac-Asp-Glu-Val-Asp-1-aldehyde (Ac-DEVD-CHO) did not block AMS101 labeling (Fig. 2C). AMS101 labeling displayed a ~45-kDa band corresponding to the mVPE in the active fraction of the chromatographic elution, indicating that mVPE has high ESENase activity (Fig. 2C). Incubation of the mVPE protein, extracted from potato TAM 24 h after BE treatment, with biotin-XVAD-fmk, and analysis of the biotinylated proteins by western blot showed one major signal at ~45 kDa (Fig. 2D), suggesting that it is the same mVPE isoform that exhibits YVADase activity as well. Taken together, these data support the notion that StVPE1 exhibits not only specificity for VPE substrate but also has caspase-1, but not caspase-3 activity.

Characterization of the optimal conditions for mVPE activity suggested its subcellular localization. mVPE, purified from potato TAM, was analyzed for ESENase activity at various pHs. Maximal ESENase activity was detected at acidic pH (4–5) (Fig. 3A). At neutral pH (7–7.5), mVPE activity was dramatically reduced to about 5% of that measured under acidic pH conditions. Accordingly, significant AMS101 labeling of mVPE was observed at pH 5.5, whereas VPE was hardly labeled at pH 7.5 (Fig. 3B). These results suggest that the acid environment in the cell vacuole is required for mVPE activity. To determine whether the potato mVPE has free thiol in the catalytic site required for activity, as has been shown to be important for VPE activity in other plants (Misas-Villamil *et al.*, 2013), we performed AMS101 labeling under reducing conditions. Withholding DTT from the reaction significantly reduced AMS101 labeling, indicating that a reducing environment is required for VPE activity (Fig. 3C).

StVPE1 is located in the TAM cell vacuole

To further examine StVPE1 protein localization within the TAM after BE treatment, we expressed the mature StVPE1 isoform containing the signal peptide (SP) and a short N-terminal propeptide, but not the auto inhibitory C-terminal domain, fused to GFP, under the control of the cauliflower mosaic virus 35S promoter (StppVPEΔC–GFP) in potato tubers. Fluorescence in the TAM was compared between BE-treated and untreated tubers (Fig. 4). StppVPEΔC–GFP fluorescence was detected, 48 h after BE treatment, at the edge of the meristem and in the procambial, early vascular tissue of the TAM (Fig. 4 B and E). In contrast, TAMs of untreated tubers showed minor VPE labeling in the leaf primordia of the meristem (Fig. 4 A and D). Within the cells, 24 h after BE treatment, StppVPEΔC–GFP was located in the

cytoplasm (Fig. 4H and 48 h after BE treatment, fluorescent aggregates of VPE were observed inside the vacuole (Fig 4I). We cannot exclude the possibility of vacuole damage at this time point, since PCD processes are expected (Teper-Bamnolker *et al.*, 2012). Twenty-one days after BE application, enhanced loss of AD was detected in three independent transgenic lines overexpressing StppVPEΔC–GFP as compared to wild-type (WT) tubers (Fig. 4 J and K).

In agreement with the increase in VPE–GFP signal and enhanced loss of AD after BE treatment, VPE activity was induced, to significantly higher levels, 48 h after BE treatment in four independent lines (Fig 4L). This observation indicated that StVPE1 overexpression is involved in loss of AD of the potato tuber.

St*VPE1* silencing prevents stem branching following BE treatment

The physiological function of St*VPE1* was further examined in seven St*VPE1*–RNAi-transgenic potato lines that showed inhibited accumulation of St*VPE* transcript levels compared to WT plants (Fig. 5A). Consistent with the reduced mRNA levels, much lower VPE activity was detected in St*VPE1*–RNAi line #6, whereas line #1 showed only a minor reduction in VPE activity as compared to the WT (Fig. 5B). AMS101 labeling displayed a 45-kDa band in the WT and St*VPE1*–RNAi line #1, but not in line #6, in agreement with the expression and activity assays (Fig. 5C). Importantly, tubers of St*VPE1*–RNAi-transgenic lines exhibited significantly increased maintenance of AD in response to BE (Fig. 5 D and E). To determine whether BE can induce secondary branching of the sprouting stems, we treated the tubers again with BE. This second application of BE to sprouting tubers caused, within 2–3 days, sprout branching from each apical stem node in the WT (Fig. 5E, bottom left). In contrast, no branching was seen in St*VPE1*–RNAi-

transgenic lines #3, #4 and #6 for up to 20 days after the additional treatment (Fig. 5E, bottom right). A specific feature of PCD is the cleavage of genomic DNA at internucleosomal sites by endogenous nucleases. To detect fragmented nuclear DNA in situ, a TUNEL procedure was applied. Exposure of WT tubers to BE for 72 h, which induces sprouting in a loss of AD manner, resulted in TUNEL-positive nuclei in the TAM (Fig. 5F). In contrast, St*VPE1*–RNAi-transgenic lines #3 and #6 showed no TUNEL staining (Fig. 5F). DNase treatment or only TUNEL labeling served as positive and negative controls, respectively. We concluded that VPE causes loss of AD in potato tubers through PCD.

DISCUSSION

Based on phylogenetic, expression and sequence analyses, VPE proteins have been classified into three categories: vegetative type, seed type and seed-coat type (Hatsugai *et al.*, 2015, Wang *et al.*, 2016, Yamada *et al.*, 2005). Potato has a vegetative-type VPE that is associated with biotic and abiotic stresses. Two vegetative-type VPE proteins have been identified in *Arabidopsis*—αVPE and γVPE—and their corresponding genes are mainly expressed in vegetative tissues. These genes are upregulated under various biotic and abiotic stresses, such as wounding, senescence, pathogen-induced hypersensitive response, and treatment with hormones such as jasmonic acid, ethylene, and salicylic acid (Albertini, Simeoni, Galbiati, Bauer, Tonelli & Cominelli, 2014, Consortium, 2011, Hara-Nishimura, Kinoshita, Hiraiwa & Nishimura, 1998, Hara-Nishimura & Maeshima, 2000, Hatsugai *et al.*, 2004, Kinoshita *et al.*, 1995a, Kinoshita, Yamada, Hiraiwa, Kondo, Nishimura & Hara-Nishimura, 1999, Yamada *et al.*, 2005). This

classification, and our previous expression study on St*VPE1*, suggest a new AD-altering role for vegetative-type VPE in the potato TAM's response to stress (Teper-Bamnolker *et al.*, 2012).

The phylogenetic analysis performed in this study showed that StVPE and SpVPE have significant similarities in their protein sequence to VPEs from other members of the Solanaceae (tobacco and tomato) (Supplementary Figs. S1 and S2). This was supported by StVPE's biochemical activity, as shown in this study.

StVPE1 is a caspase-1-like enzyme that is localized to the cell vacuole of the TAM

Decapitation of the apical bud causes immediate loss of AD in potato tuber (reviewed by Cline, 1997, Teper-Bamnolker *et al.*, 2012). It is likely that external stresses affect the viability of the apical meristem and/or some of its cells, which in turn affects the strength of its dominance. We previously reported that loss of AD, induced by either long cold storage or BE treatment, is correlated with the occurrence of PCD in the TAM, suggesting a functional relationship between local PCD and AD control through an effect on TAM cell viability (Teper-Bamnolker *et al.*, 2012). We also showed that treatment with BE, which causes sprouting accompanied by loss of AD, induces VPE activity in the TAM (Teper-Bamnolker *et al.*, 2012). The specific labeling of mVPE by AMS101 only after BE treatment confirmed its identity as the mature active form of StVPE1, induced by BE treatment (Fig. 2A).

StVPE1 exhibited VPE-specific activity (ESENase and YVADase), similar to *Arabidopsis* VPEs (Cai & Gallois, 2015, Kuroyanagi *et al.*, 2005), suggesting its role in destructive PCD in potato TAM (Fig. 2B). The efficiency of the caspase-1 inhibitor Ac-YVAD-CHO's inhibition of YVADase activity and prevention of AMS101 labeling

supported its caspase-1-like function (Fig. 2 B and C). In contrast, the purified mVPE displayed almost no caspase-3 activity (DEVDase; Fig. 2B). Accordingly, no prevention of AMS101 labeling by the caspase-3 inhibitor Ac-DEVD-CHO was detected (Fig. 2C).

VPE is a vacuolar enzyme (Hara-Nishimura & Maeshima, 2000, Hatsugai *et al.*, 2015, Kinoshita *et al.*, 1999) and consequently, it exhibits maximal activity at acidic pH (Fig. 3A), suggesting optimal localization for activity in the cell vacuole (Hatsugai *et al.*, 2006, Kinoshita *et al.*, 1999, Kuroyanagi *et al.*, 2002, Mino *et al.*, 2007, Misas-Villamil *et al.*, 2013, Sueldo & van der Hoorn, 2017). VPE is a legumain, a member of the cysteine proteases (reviewed by Bonneau, Ge, Drury & Gallois, 2008, Bosch, Poulter, Perry, Wilkins & Franklin-Tong, 2010). Other legumains, such as pig legumain, can also cleave the caspase-1 substrate Ac-YVAD-AMC, with maximum activity at pH 5.0 (Rotari, Dando & Barrett, 2001). The self-catalytic maturation and activation of recombinant *Arabidopsis* VPEγ has been shown to occur *in vitro* under acidic conditions (Kuroyanagi *et al.*, 2002). This implies that the vegetative VPE precursor is transported to the vacuole where it is converted into its active mature form, and regulates the activation of some functional proteins in the lytic vacuoles (Kinoshita *et al.*, 1999).

StppVPEΔC–GFP was localized to the meristem tip and vascular tissue of the TAM (Fig. 4B). Within the cell, it was localized to the cytoplasm and the lumen of the vacuole (Fig. 4 E and F), leading to enhanced loss of tuber AD compared to the WT (Fig. 4 J and K). Vacuolar localization of VPE was previously demonstrated for the *Arabidopsis* vegetative VPEγ (Kinoshita *et al.*, 1999), and later confirmed by live imaging using AMS101, which revealed mobile fluorescent speckles inside the vacuole but not in the nucleus or cytoplasm (Misas-Villamil *et al.*, 2013). Our results

suggest that VPE is expressed in the cytoplasm endoplasmic reticulum (ER), since it is equipped with a signal peptide; after BE treatment, it translocates to the central vacuole to form stable aggregates (Fig. 4 H and I). Although we used the 35S promotor, StVPEΔC–GFP signal and VPE activity only increased after BE treatment (Fig. 4 A–I), suggesting higher stability of VPE induced by BE, probably via translocation and aggregation.

VPEs that exhibit caspase-1-like activity play important roles in different types of PCD as a vacuolar protease involved in maturation of vacuolar proteins (Hara-Nishimura, Inoue & Nishimura, 1991, Kinoshita, Nishimura & Hara-Nishimura, 1995b, Wang *et al.*, 2016). The potato vegetative VPE1 is activated by external stress in plant vegetative tissue, leading to its translocation to the central vacuole where acid conditions allow its caspase-1-like activity.

St*VPE1* silencing reduces stem branching

The physiological function of St*VPE1* was examined using seven St*VPE1*–RNAi-transgenic potato lines. The differential response to BE treatment, as compared to the WT-treated tubers, suggests that abiotic stress is required to activate StVPE1 in the TAM. A correlation was found between the degree of reduction in St*VPE1* expression in St*VPE*1–RNAi-transgenic lines, VPE activity and maintenance of AD (Fig. 5). We suggest that VPE is involved in inducing destructive PCD in the TAM that probably results in viability loss resembling the decapitation known to induce loss of AD (Teper-Bamnolker *et al.*, 2012). In our experience, BE can affect any exposed bud, apical or lateral, and reduce its dominance, even on the same tuber node ("eye"), as evidenced by the observed secondary branching of stems after second application of BE (Fig. 5E). The TAM is probably most affected because it is

the most exposed tissue and the first to undergo bud burst when dormancy is released. A similar function for VPE has been shown in the hypersensitive response to viruses and fungal toxins, and in developmental cell death to generate integuments (seed coats) and tracheary elements (reviewed by Hara-Nishimura & Hatsugai, 2011, Minina, Smertenko & Bozhkov, 2014). The St*VPE1*–RNAi-transgenic potato's lack of response to BE indicates a functional relationship between VPE activity and cell death in the TAM. We suggest that BE is a chemical stress that induces StVPE1 enzyme activation followed by PCD in the apical meristem, leading to partial decapitation of the TAM and loss of AD.

ACKNOWLEDGMENTS

This research was funded by a grant from the Chief Scientist of the Ministry of Agriculture and Rural Development of Israel (no. 132174113). The manuscript is a contribution of the Agricultural Research Organization, the Volcani Center, Rishon LeZion, Israel, no. 701/14.

The authors thank Professor Robert Fluhr, from the Department of Plant Sciences, Weizmann Institute of Science, for his valuable suggestions and constructive criticism.

REFERENCES

Albertini A., Simeoni F., Galbiati M., Bauer H., Tonelli C. & Cominelli E. (2014) Involvement of the vacuolar processing enzyme γVPE in response of Arabidopsis thaliana to water stress. *Biologia plantarum*, **58**, 531-538.

Alexopoulos A.A., Aivalakis G., Akoumianakis K.A. & Passam H.C. (2009) Bromoethane induces dormancy breakage and metabolic changes in tubers derived from true potato seed. *Postharvest Biol Technol*, **54**, 165 - 171.

Altschul S.F., Madden T.L., Schäffer A.A., Zhang J., Zhang Z., Miller W. & Lipman D.J. (1997) Gapped BLAST and PSI-BLAST: a new generation of protein database search programs. *Nucleic Acids Res*, **25**, 3389-3402.

Bonneau L., Ge Y., Drury G.E. & Gallois P. (2008) What happened to plant caspases? *J Exp Bot*, **59**, 491 -499.

Bosch M., Poulter N.S., Perry R.M., Wilkins K.A. & Franklin-Tong V.E. (2010) Characterization of a legumain/vacuolar processing enzyme and YVADase activity in Papaver pollen. *Plant molecular biology*, **74**, 381-393.

Burton W.G. (1989) *The Potato*. Longman Scientific, Harlow, England.

Buskila Y., Sela N., Teper-Bamnolker P., Tal I., Shani E., Weinstain R., Gaba V., Tam Y., Lers A. & Eshel D. (2016) Stronger sink demand for metabolites supports dominance of the apical bud in etiolated growth. *Journal of experimental botany*, erw315.

Cai Y.-m. & Gallois P. (2015) Programmed Cell Death Regulation by Plant Proteases with Caspase-Like Activity. In: *Plant Programmed Cell Death*, pp. 191-202. Springer.

Campbell M., Segear E., Beers L., Knauber D. & Suttle J. (2008) Dormancy in potato tuber meristems: chemically induced cessation in dormancy matches the natural process based on transcript profiles. *Funct Integr Genom*, **8**, 317-328.

Cline M. (1997) Concepts and terminology of apical dominance. *American J Bot*, **84**, 1064-1064.

Consortium P.G.S. (2011) Genome sequence and analysis of the tuber crop potato. *Nature*, **475**, 189-195.

Destefano-Beltran L., Knauber D., Huckle L. & Suttle J. (2006) Chemically forced dormancy termination mimics natural dormancy progression in potato tuber meristems by reducing ABA content and modifying expression of genes involved in regulating ABA synthesis and metabolism. *J Exp Bot*, **57**, 2879-2886.

Eshel D. (2015) Bridging Dormancy Release and Apical Dominance in Potato Tuber. In: *Advances in Plant Dormancy*, pp. 187-196. Springer.

Eshel D. & Teper-Bamnolker P. (2012) Can loss of apical dominance in potato tuber serve as a marker of physiological age? *Plant Signaling & Behavior*, **7**, 1158-1162.

Gleave A.P. (1992) A versatile binary vector system with a T-DNA organisational structure conducive to efficient integration of cloned DNA into the plant genome. *Plant Mol Biol*, **20**, 1203-1207.

Guindon S., Dufayard J.-F., Lefort V., Anisimova M., Hordijk W. & Gascuel O. (2010) New algorithms and methods to estimate maximum-likelihood phylogenies: assessing the performance of PhyML 3.0. *Systematic biology*, **59**, 307-321.

Gunawardena A. & McCabe P.F. (2015) *Plant programmed cell death*. Springer.

Hara-Nishimura I. & Hatsugai N. (2011) The role of vacuole in plant cell death. *Cell Death Differ*, **18**, 1298-1304.

Hara-Nishimura I., Inoue K. & Nishimura M. (1991) A unique vacuolar processing enzyme responsible for conversion of several proprotein precursors into the mature forms. *FEBS lett*, **294**, 89-93.

Hara-Nishimura I., Kinoshita T., Hiraiwa N. & Nishimura M. (1998) Vacuolar processing enzymes in protein-storage vacuoles and lytic vacuoles. *J Plant Physiol*, **152**, 668-674.

Hara-Nishimura I. & Maeshima M. (2000) Vacuolar processing enzymes and aquaporins. *Ann Plant Rev*, **5**, 20-42.

Hatsugai N., Kuroyanagi M., Nishimura M. & Hara-Nishimura I. (2006) A cellular suicide strategy of plants: vacuole-mediated cell death. *Apoptosis*, **11**, 905 -911.

Hatsugai N., Kuroyanagi M., Yamada K., Meshi T., Tsuda S., Kondo M., Nishimura M. & Hara-Nishimura I. (2004) A plant vacuolar protease, VPE, mediates virus-induced hypersensitive cell death. *Science*, **305**, 855-858.

Hatsugai N., Yamada K., Goto-Yamada S. & Hara-Nishimura I. (2015) Vacuolar processing enzyme in plant programmed cell death. *Frontiers in plant science*, **6**, 234.

Horsch R., Rogers S. & Fraley R. (1985) *Transgenic plants*. Paper presented at the Cold Spring Harbor symposia on quantitative biology.

Kabbage M., Kessens R., Bartholomay L.C. & Williams B. (2017) The Life and Death of a Plant Cell. *Annual Review of Plant Biology*, **68**.

Karimi M., Depicker A. & Hilson P. (2007) Recombinational cloning with plant gateway vectors. *Plant Physiology*, **145**, 1144-1154.

Kinoshita T., Nishimura M. & Hara-Nishimura I. (1995a) Homologues of a vacuolar processing enzyme that are expressed in different organs in *Arabidopsis thaliana*. *Plant Mol Biol*, **29**, 81-89.

Kinoshita T., Nishimura M. & Hara-Nishimura I. (1995b) The sequence and expression of the γ-VPE gene, one member of a family of three genes for vacuolar processing enzymes in *Arabidopsis thaliana*. *Plant Cell Physiol*, **36**, 1555-1562.

Kinoshita T., Yamada K., Hiraiwa N., Kondo M., Nishimura M. & Hara-Nishimura I. (1999) Vacuolar processing enzyme is up-regulated in the

lytic vacuoles of vegetative tissues during senescence and under various stressed conditions. *Plant J*, **19**, 43-53.

Kuroyanagi M., Nishimura M. & Hara-Nishimura I. (2002) Activation of Arabidopsis vacuolar processing enzyme by self-catalytic removal of an auto-inhibitory domain of the C-terminal propeptide. *Plant Cell Physiol*, **43**, 143-151.

Kuroyanagi M., Yamada K., Hatsugai N., Kondo M., Nishimura M. & Hara-Nishimura I. (2005) Vacuolar processing enzyme is essential for mycotoxin-induced cell death in *Arabidopsis thaliana*. *J Biol Chem*, **280**, 32914-32920.

Law R.D. & Suttle J.C. (2003) Transient decreases in methylation at 5'-CCGG-3' sequences in potato (*Solanum tuberosum* L.) meristem DNA during progression of tubers through dormancy precede the resumption of sprout growth. *Plant Mol Biol*, **51**, 437-447.

Le S.Q. & Gascuel O. (2008) An improved general amino acid replacement matrix. *Molecular biology and evolution*, **25**, 1307-1320.

Lu H., Chandrasekar B., Oeljeklaus J., Misas-Villamil J.C., Wang Z., Shindo T., Bogyo M., Kaiser M. & van der Hoorn R.A. (2015) Subfamily-specific fluorescent probes for cysteine proteases display dynamic protease activities during seed germination. *Plant physiology*, **168**, 1462-1475.

Minina E.A., Smertenko A.P. & Bozhkov P.V. (2014) Vacuolar cell death in plants. *Autophagy*, **10**, 1-2.

Mino M., Murata N., Date S. & Inoue M. (2007) Cell death in seedlings of the interspecific hybrid of *Nicotiana gossei* and *N. tabacum*; possible role of knob-like bodies formed on tonoplast in vacuolar-collapse-mediated cell death. *Plant Cell Rep*, **26**, 407–419.

Misas-Villamil J.C., Toenges G., Kolodziejek I., Sadaghiani A.M., Kaschani F., Colby T., Bogyo M. & Hoorn R.A. (2013) Activity profiling of vacuolar processing enzymes reveals a role for VPE during oomycete infection. *The Plant J*, **73**, 689-700.

Nakaune S., Yamada K., Kondo M., Kato T., Tabata S., Nishimura M. & Hara-Nishimura I. (2005) A vacuolar processing enzyme, δVPE, is involved in seed coat formation at the early stage of seed development. *Plant Cell*, **17**, 876-887.

Rocha-Sosa M., Sonnewald U., Frommer W., Stratmann M., Schell J. & Willmitzer L. (1989) Both developmental and metabolic signals activate the promoter of a class I patatin gene. *EMBO J*, **8**, 23-29.

Rotari V.I., Dando P.M. & Barrett A.J. (2001) Legumain forms from plants and animals differ in their specificity. *Biol Chem*, **382**, 953-959.

Shimada T., Yamada K., Kataoka M., Nakaune S., Koumoto Y., Kuroyanagi M., Tabata S., Kato T., Shinozaki K. & Seki M. (2003) Vacuolar processing enzymes are essential for proper processing of seed storage proteins in *Arabidopsis thaliana*. *J Biol Chem*, **278**, 32292-32299.

Sonnewald S. & Sonnewald U. (2014) Regulation of potato tuber sprouting. *Planta*, **239**, 27-38.

Sueldo D.J. & van der Hoorn R.A. (2017) Plant life needs cell death, but does plant cell death need Cys proteases? *The FEBS Journal*.

Suttle J.C. (2004) Physiological regulation of potato tuber dormancy. *Am J Potato Res*, **81**, 253-262.

Teper-Bamnolker P., Buskila Y., Lopesco Y., Ben-Dor S., Saad I., Holdengreber V., Belausov E.d., Zemach H., Ori N., Lers A. & Eshel D. (2012) Release of apical dominance in potato tuber is accompanied by programmed cell death in the apical bud meristem. *Plant Physiol*, **158**, 2053-2067.

Teper-Bamnolker P., Dudai N., Fischer R., Belausov E., Zemach H., Shoseyov O. & Eshel D. (2010) Mint essential oil can induce or inhibit potato sprouting by differential alteration of apical meristem. *Planta*, **232**, 179–186.

van der Hoorn R.A. & Kaiser M. (2012) Probes for activity-based profiling of plant proteases. *Physiol Plantarum*, **145**, 18-27.

Van Hautegem T., Waters A.J., Goodrich J. & Nowack M.K. (2015) Only in dying, life: programmed cell death during plant development. *Trends in plant science*, **20**, 102-113.

Wang N., Duhita N., Ariizumi T. & Ezura H. (2016) Involvement of vacuolar processing enzyme SlVPE5 in post-transcriptional process of invertase in sucrose accumulation in tomato. *Plant Physiol Biochem*, **108**, 71-78.

Wang W., Cai J., Wang P., Tian S. & Qin G. (2017) Post-transcriptional regulation of fruit ripening and disease resistance in tomato by the vacuolar protease SlVPE3. *Genome biology*, **18**, 47.

Weigel D. & Glazebrook J. (2006) Transformation of Agrobacterium using electroporation. *Cold Spring Harb Protoc*, **2006**, 4665.

Wesley S.V., Helliwell C.C., Smith N.A., Wang M., Rouse D.T., Liu Q., Gooding P.S., Singh S.P., Abbott D., Stoutjesdijk P.A., Robinson S.P., Gleave A.P., Green A.G. & Waterhouse P.M. (2001) Construct design for efficient, effective and high-throughput gene silencing in plants. *The Plant J.*, **27**, 581-590.

Yamada K., Shimada T., Nishimura M. & Hara-Nishimura I. (2005) A VPE family supporting various vacuolar functions in plants. *Physiol Plantarum*, **123**, 369-375.

SUPPORTING INFORMATION

Additional supporting information may be found in the online version of this article.

Table S1. Genomic Loci and Gene Models in Potato and Tomato.

Fig. S1. Predicted amino acid sequences of VPE from *Solanum tuberosum* (St), *Solanum phureja* (Sp), *Solanum lycopersicon* (Sl), and *Nicotiana tabacum* (Nt).

Fig. S2. Multiple sequence alignment of VPE from *Solanum tuberosum* (St), *Solanum phureja* (Sp), *Solanum lycopersicon* (Sl), and *Nicotiana tabacum* (Nt). Protein sequences were aligned using the MAFFT program (http://mafft.cbrc.jp/alignment/server/ version 7). Indicated are catalytic dyad (red), three crucial amino acids which form the substrate pocket (blue), propeptides of StVPE1 (bold) and the green fluorescent protein (GFP) fusion site (Hatsugai *et al.*, 2006, van der Hoorn & Kaiser, 2012).

FIGURE LEGENDS

Fig. 1. *StVPE1* is a vegetative-type VPE. (A) Structure of VPE genomic loci in *Solanum phureja* (Sp) and *Solanum lycopersicum* (Sl). Gray lines connect highest BLAST hits between *S. phureja* and *S. lycopersicum*. Different colors represent VPE types as explained in B. (B) Phylogenetic analysis of *VPE* from *Solanum tuberosum* (St), *S. phureja* (Sp) indicated in blue color, *S. lycopersicum* (Sl) and *Nicotiana tabacum* (Nt). Plant VPE proteins were classified based on their protein sequences into four branches and three types—vegetative type (g, gray), seed type (b, blue) and seed-coat type (d, green). Phylogenetic analyses were conducted using the MAFFT program and maximum likelihood method (PhyML 3.0 software). The neighbor-joining tree is shown. The accession numbers are indicated in parentheses. VPE protein sequences can be found in Supplementary Fig. S1. *StVPE1* is indicated in purple.

Fig. 2. Bromoethane (BE) treatment induces higher expression of St*VPE1* mature protein (mVPE) in the tuber apical meristem (TAM) with caspase-like activity. (A) AMS101 labeling of the mVPE in the cell extract of the TAM 24, 48 and 72 h after BE treatment as compared to nontreated tubers. (B) The partially purified mVPE was tested for its substrate specificity using the VPE-specific substrate Ac-ESEN-MCA, and for caspase-1- and caspase-3-like activities using Ac-YVAD-MCA and Ac-DEVD-MCA substrates, respectively. The effect of the caspase-1 specific inhibitor Ac-YVAD-CHO on VPEase and caspase relative activities was calculated as well. Substrate and inhibitor effects were expressed as percentage of the activity

obtained using Ac-ESEN-MCA without inhibitor. Error bars represent standard error of the mean (SE) of three repeats, n = 5. Different letters denote significant effect of the inhibitor in each substrate ($P < 0.05$). (C) Caspase-1 (Ac-YVAD-CHO) but not caspase-3 (Ac-DEVD-CHO) inhibitors suppress mVPE labeling by AMS101. Protein extracts from TAM were preincubated for 30 min with 300 μM caspase-1 or caspase-3 inhibitor, followed by 2 h labeling with 1.5 μM AMS101. (D) mVPE extracted from potato TAM 24 h after BE treatment was labeled with biotin-XVAD-fmk. The biotinylated protein band was detected by immunoblot using horseradish peroxidase-conjugated streptavidin.

Fig. 3. Mature (m) VPE extracted from tuber apical meristem (TAM) 24 h after bromoethane (BE) treatment is active at acidic pH and under reducing conditions. (A) mVPE activity under different pHs. The comparison was made using citrate phosphate buffers with a range of pHs (4–7.5). Activity was measured using the substrate Ac-ESEN-MCA. Error bars represent SE of three repeats, n = 5. Different letters denote significant differences ($P < 0.05$). (B) Acidic conditions increase mVPE substrate binding. AMS101 labeling of mVPE at pH 5.5 as compared to pH 7.5. (C) Reducing conditions induce the formation of the active mVPE isoform. Proteins were labeled at pH 5.5 for 2 h with 1.5 μM AMS101 with or without 10 mM DTT.

Fig. 4. StppVPEΔC–GFP is localized to the cell vacuole in tuber apical meristem (TAM) after bromoethane (BE) treatment. (A, D and G) StppVPEΔC–GFP localization within the TAM cells of nontreated tubers after 72 h of incubation, (B, E,

and H) 24 h after BE treatment or (C, F and I) 48 h after BE treatment. Note that within the TAM, StVPEΔC–GFP labeling is localized to the meristem tip (E and F, a close-up of the meristem tip and in the procambial, early vascular tissue of the TAM (B)). Within the cell, VPE has accumulated in the cytoplasm 24 h after BE treatment (H) and is then 48h after treatment detected as aggregates within the vacuole (I). Abbreviations: am, apical meristem; lp, leaf primordia; pc, procambium; v, vacuole. Arrowheads show examples of StVPEΔC–GFP aggregates. (J and K) Enhanced loss of tuber AD due to VPE overexpression, represented by number of sprouts in each tuber, 21 days after BE treatment, shown in three independent transgenic lines (#9, #12 and #16) as compared to the WT. Five tubers from each plant and three plants from each transgenic line were analyzed in each treatment. Error bars represent standard error of the mean (SE). Different letters denote significant differences for each transgenic line ($P < 0.05$). (L) VPE activity in the overexpressed line without BE treatment and 48 h after BE treatment. Data represent averages ± SE of three repeats, n = 5. Different uppercase letters denote significant differences for each transgenic line between treatments (+/- BE); different lowercase letters denote significant differences for each treatment (+/- BE) between transgenic lines ($P < 0.05$).

Fig. 5. StVPE1 silencing prevents stem branching following BE treatment. (A) Quantitative PCR analysis of seven St*VPE*–RNAi-transgenic plants (#1 to #6) as compared to wild-type (WT) cv. Désirée, 72 h after BE treatment. (B) VPE activity in leaves of St*VPE*–RNAi lines #1 and #6, 72 h after BE treatment, measured by using the VPE-specific substrate Ac-ESEN-MCA. (C) AMS101 labeling of StVPE in leaf extract of St*VPE*–RNAi lines #1 and #6 as compared to WT plants, 72 h after BE

treatment. (D) Delayed loss of tuber AD in StVPE1–RNAi lines, represented by number of sprouts in each tuber, 10 days after BE treatment, shown in three transgenic lines (#3, #4 and #6) as compared to the WT. Error bars represent standard error of the mean (SE) of three repeats. Different letters denote significant differences for each transgenic line ($P < 0.05$). (E) Three representative tubers of St*VPE*–RNAi line #6 compared to three WT tubers, treated with BE before (upper panels) and again after (lower panel) sprouting. Five tubers from each plant and three plants from each transgenic line, were analyzed in each treatment. Representative pictures were taken 10 days after each treatment. Bars = 2 cm. (F) DNA fragmentation in tuber apical meristems (TAMs) of WT and St*VPE1*–RNAi lines #3 and #6, 72 h after BE treatment. Histological analyses were performed on 10-µm thick TAM sections. The cells were counterstained in situ with DAPI (blue color represents nuclei) followed by TUNEL reagents (green color represents DNA fragmentation). Corresponding phase-contrast images (PhC) of meristem tissue are also shown. Bars = 50 µm.

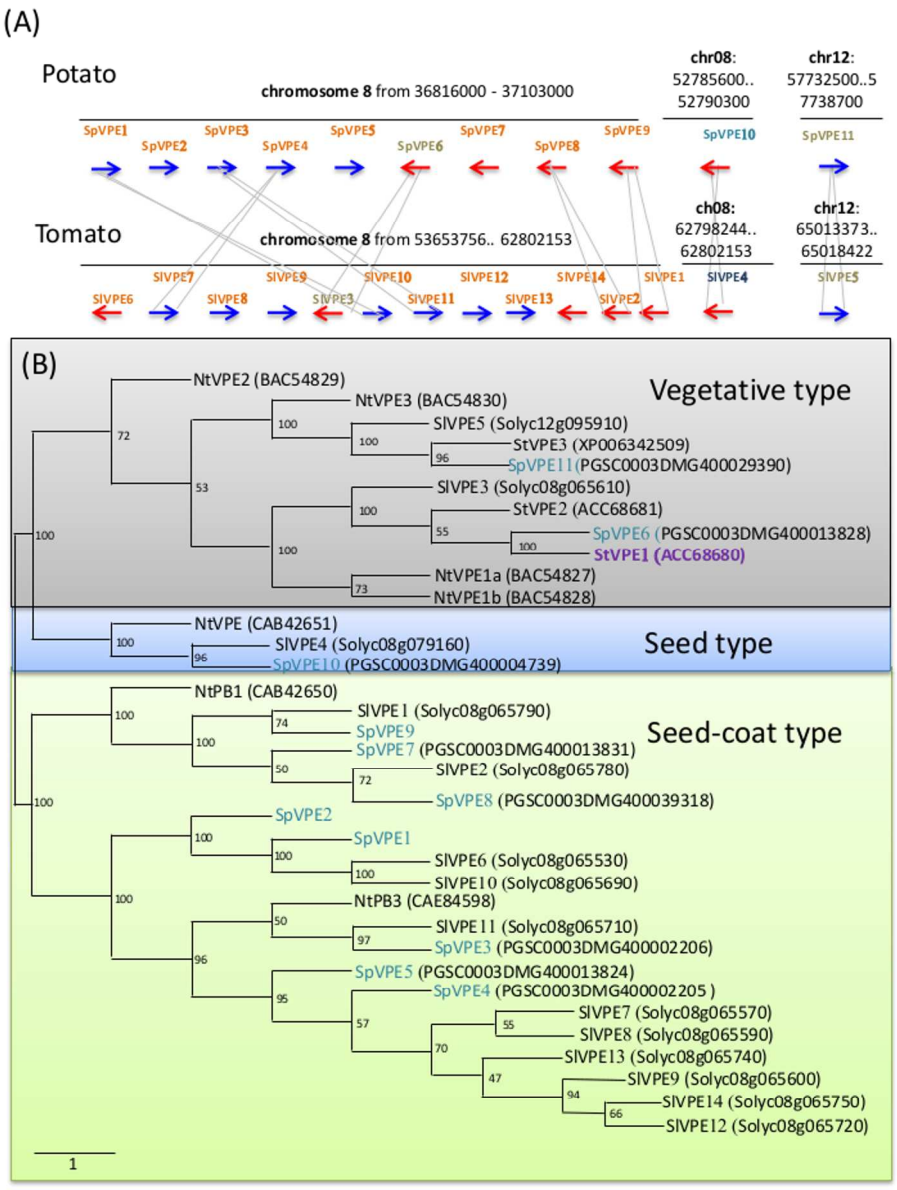

Fig. 1. *StVPE1* is a vegetative-type VPE. (A) Structure of VPE genomic loci in *Solanum phureja* (Sp) and *Solanum lycopersicum* (Sl). Gray lines connect highest BLAST hits between *S. phureja* and *S. lycopersicum*. Different colors represent VPE types as explained in B. (B) Phylogenetic analysis of VPE from *Solanum tuberosum* (St), *S. phureja* (Sp) indicated in blue color, *S. lycopersicum* (Sl) and *Nicotiana tabacum* (Nt). Plant VPE proteins were classified based on their protein sequences into four branches and three types—vegetative type (g, gray), seed type (b, blue) and seed-coat type (d, green). Phylogenetic analyses were conducted using the MAFFT program and maximum likelihood method (PhyML 3.0 software). The neighbor-joining tree is shown. The accession numbers are indicated in parentheses. VPE protein sequences can be found in Supplementary Fig. S1. *StVPE1* is indicated in purple.

219x283mm (300 x 300 DPI)

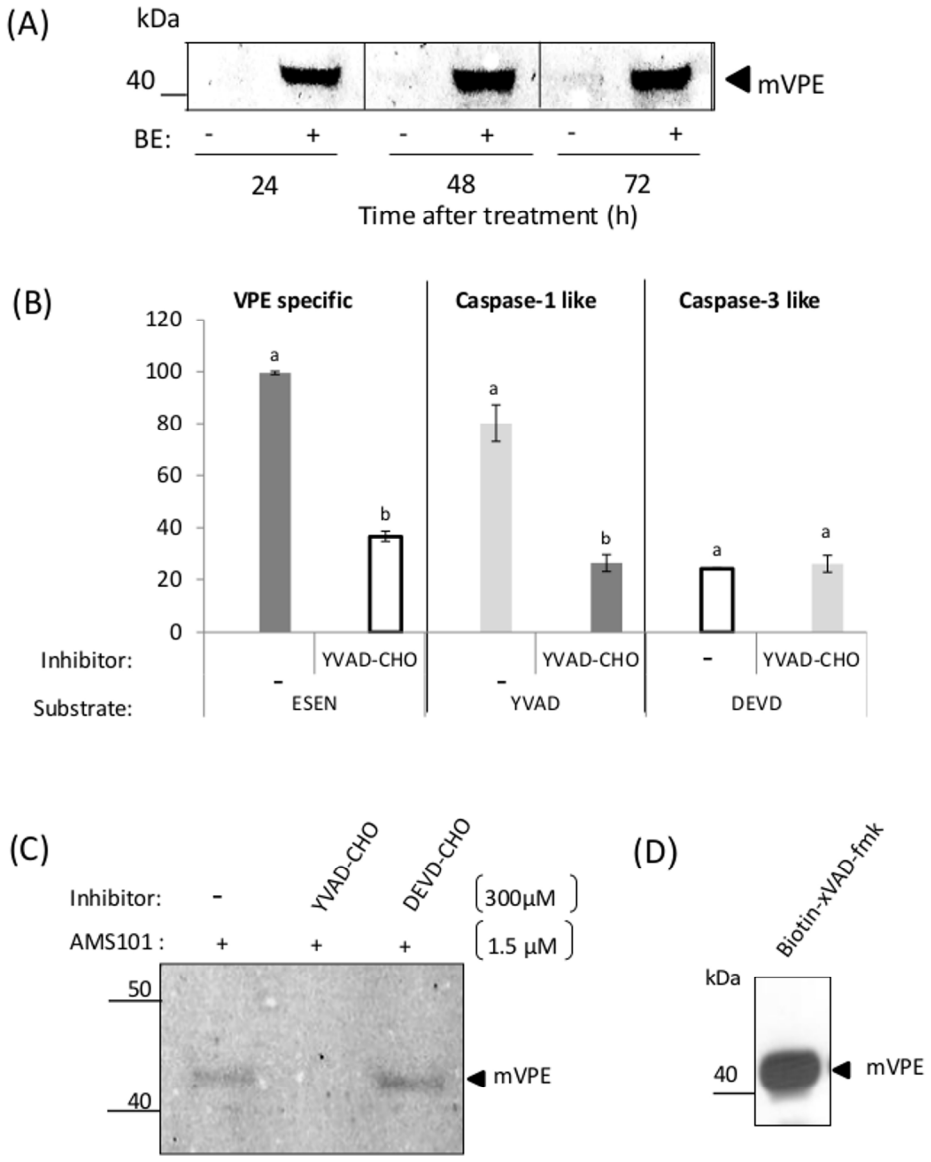

Fig. 2. Bromoethane (BE) treatment induces higher expression of StVPE1 mature protein (mVPE) in the tuber apical meristem (TAM) with caspase-like activity. (A) AMS101 labeling of the mVPE in the cell extract of the TAM 24, 48 and 72 h after BE treatment as compared to nontreated tubers. (B) The partially purified mVPE was tested for its substrate specificity using the VPE-specific substrate Ac-ESEN-MCA, and for caspase-1- and caspase-3-like activities using Ac-YVAD-MCA and Ac-DEVD-MCA substrates, respectively. The effect of the caspase-1 specific inhibitor Ac-YVAD-CHO on VPEase and caspase relative activities was calculated as well. Substrate and inhibitor effects were expressed as percentage of the activity obtained using Ac-ESEN-MCA without inhibitor. Error bars represent standard error of the mean (SE) of three repeats, n = 5. Different letters denote significant effect of the inhibitor in each substrate ($P < 0.05$). (C) Caspase-1 (Ac-YVAD-CHO) but not caspase-3 (Ac-DEVD-CHO) inhibitors suppress mVPE labeling by AMS101. Protein extracts from TAM were preincubated for 30 min with 300 µM caspase-1 or caspase-3 inhibitor, followed by 2 h labeling with 1.5 µM AMS101. (D) mVPE extracted from potato TAM 24 h after BE treatment was labeled with biotin-XVAD-fmk. The biotinylated protein band was detected by immunoblot using horseradish

peroxidase-conjugated streptavidin.

214x270mm (300 x 300 DPI)

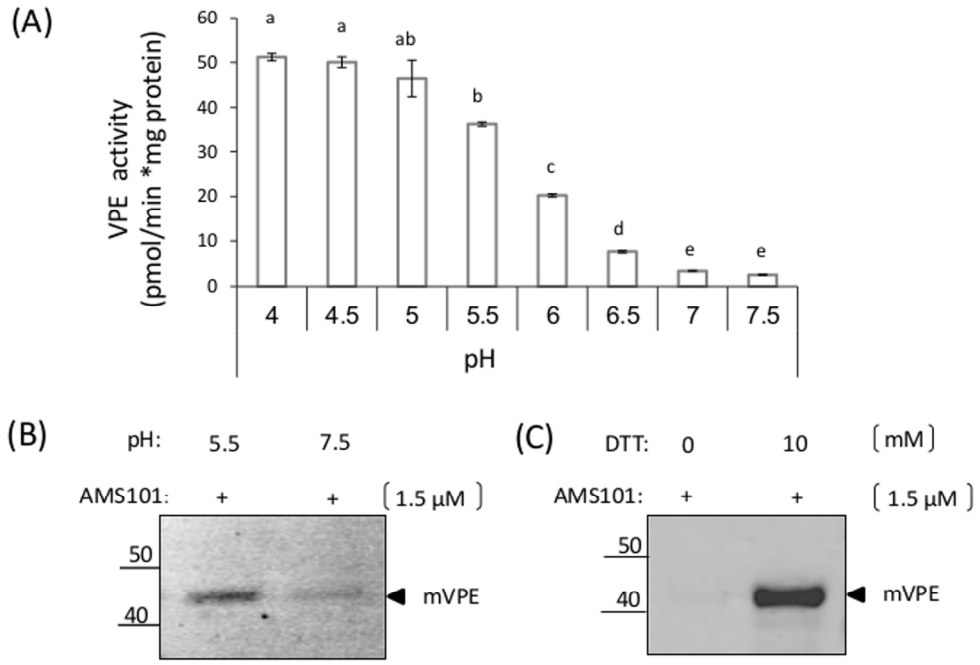

Fig. 3. Mature (m) VPE extracted from tuber apical meristem (TAM) 24 h after bromoethane (BE) treatment is active at acidic pH and under reducing conditions. (A) mVPE activity under different pHs. The comparison was made using citrate phosphate buffers with a range of pHs (4–7.5). Activity was measured using the substrate Ac-ESEN-MCA. Error bars represent SE of three repeats, n = 5. Different letters denote significant differences ($P < 0.05$). (B) Acidic conditions increase mVPE substrate binding. AMS101 labeling of mVPE at pH 5.5 as compared to pH 7.5. (C) Reducing conditions induce the formation of the active mVPE isoform. Proteins were labeled at pH 5.5 for 2 h with 1.5 µM AMS101 with or without 10 mM DTT.

129x98mm (300 x 300 DPI)

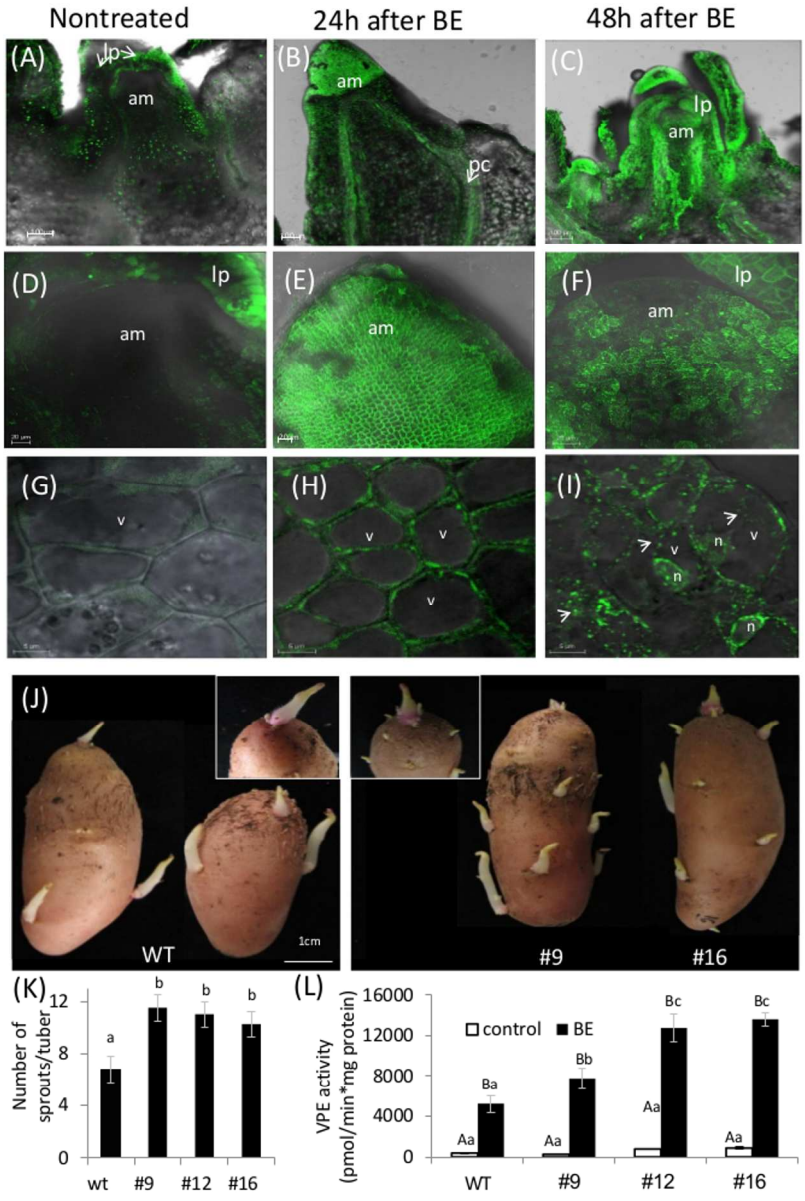

Fig. 4. StppVPEΔC–GFP is localized to the cell vacuole in tuber apical meristem (TAM) after bromoethane (BE) treatment. (A, D and G) StppVPEΔC–GFP localization within the TAM cells of nontreated tubers after 72 h of incubation, (B, E, and H) 24 h after BE treatment or (C, F and I) 48 h after BE treatment. Note that within the TAM, StVPEΔC–GFP labeling is localized to the meristem tip (E and F, a close-up of the meristem tip and in the procambial, early vascular tissue of the TAM (B)). Within the cell, VPE has accumulated in the cytoplasm 24 h after BE treatment (H) and is then 48h after treatment detected as aggregates within the vacuole (I). Abbreviations: am, apical meristem; lp, leaf primordia; pc, procambium; v, vacuole. Arrowheads show examples of StVPEΔC–GFP aggregates. (J and K) Enhanced loss of tuber AD due to VPE overexpression, represented by number of sprouts in each tuber, 21 days after BE treatment, shown in three independent transgenic lines (#9, #12 and #16) as compared to the WT. Five tubers from each plant and three plants from each transgenic line were analyzed in each treatment. Error bars represent standard error of the mean (SE). Different letters denote significant differences for each transgenic line ($P < 0.05$). (L) VPE activity in the overexpressed line without BE treatment and 48 h after BE treatment. Data represent

averages ± SE of three repeats, n = 5. Different uppercase letters denote significant differences for each transgenic line between treatments (+/- BE); different lowercase letters denote significant differences for each treatment (+/- BE) between transgenic lines ($P < 0.05$).

249x366mm (300 x 300 DPI)

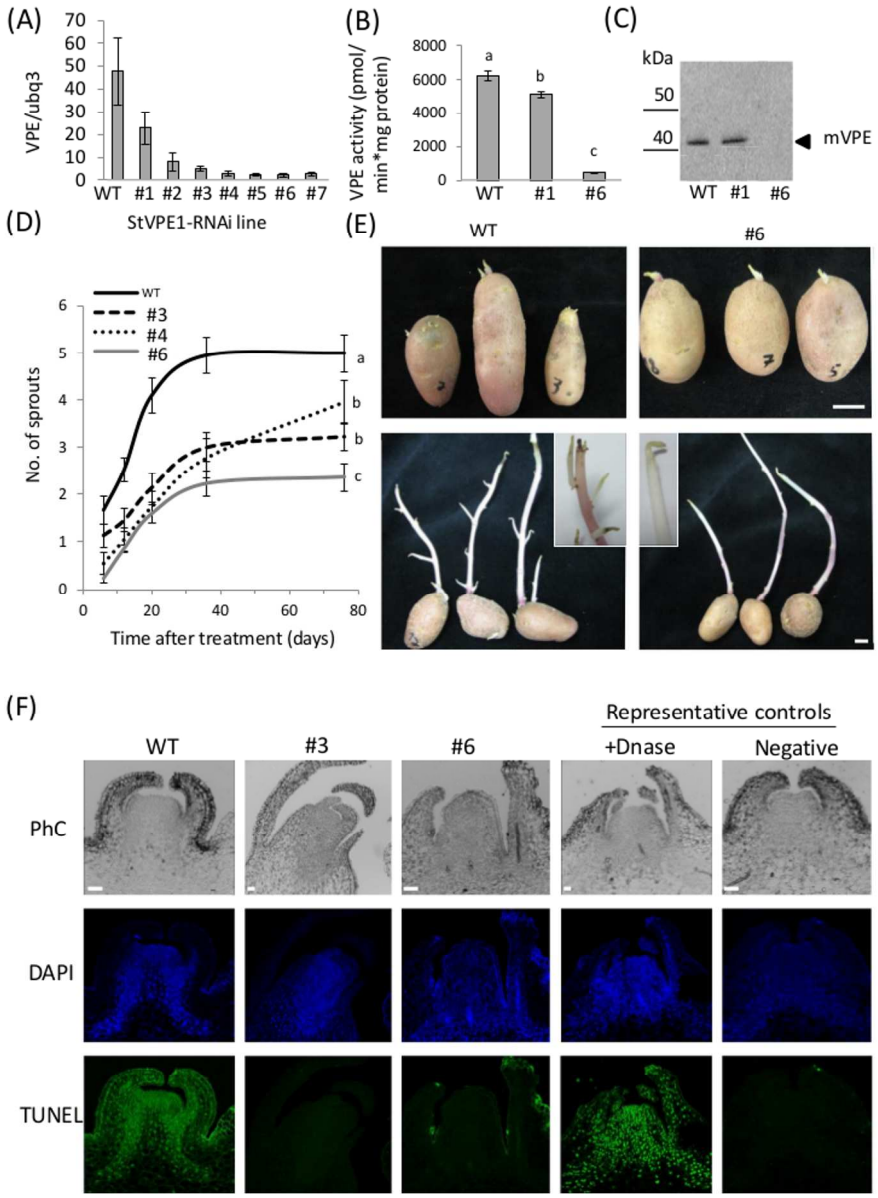

Fig. 5. StVPE1 silencing prevents stem branching following BE treatment. (A) Quantitative PCR analysis of seven StVPE–RNAi-transgenic plants (#1 to #6) as compared to wild-type (WT) cv. Désirée, 72 h after BE treatment. (B) VPE activity in leaves of StVPE–RNAi lines #1 and #6, 72 h after BE treatment, measured by using the VPE-specific substrate Ac-ESEN-MCA. (C) AMS101 labeling of StVPE in leaf extract of StVPE–RNAi lines #1 and #6 as compared to WT plants, 72 h after BE treatment. (D) Delayed loss of tuber AD in StVPE1–RNAi lines, represented by number of sprouts in each tuber, 10 days after BE treatment, shown in three transgenic lines (#3, #4 and #6) as compared to the WT. Error bars represent standard error of the mean (SE) of three repeats. Different letters denote significant differences for each transgenic line ($P < 0.05$). (E) Three representative tubers of StVPE–RNAi line #6 compared to three WT tubers, treated with BE before (upper panels) and again after (lower panel) sprouting. Five tubers from each plant and three plants from each transgenic line, were analyzed in each treatment. Representative pictures were taken 10 days after each treatment. Bars = 2 cm. (F) DNA fragmentation in tuber apical meristems (TAMs) of WT and StVPE1–RNAi lines #3 and #6, 72 h after BE treatment. Histological analyses were performed on 10-µm

thick TAM sections. The cells were counterstained in situ with DAPI (blue color represents nuclei) followed by TUNEL reagents (green color represents DNA fragmentation). Corresponding phase-contrast images (PhC) of meristem tissue are also shown. Bars = 50 μm.

228x308mm (300 x 300 DPI)